

# Review of surface metrology artifacts for additive manufacturing

Patryk Mietliński<sup>1</sup>, Bartosz Gapiński<sup>1</sup>, Jolanta B. Królczyk<sup>2</sup>, Piotr Niesłony<sup>2</sup>, Marta Bogdan-Chudy<sup>2</sup>, Anna Trych-Wildner<sup>3</sup>, Natalia Wojciechowska<sup>3</sup>, Grzegorz M. Królczyk<sup>2</sup>, Michał Wieczorowski<sup>1</sup>, Tomasz Bartkowiak<sup>1\*</sup>

<sup>1</sup>Poznan University of Technology, Poland

<sup>2</sup>Opole University of Technology, Poland

<sup>3</sup>Central Office of Measures (GUM), Poland

**Abstract** Test artifacts, resembling real machine parts, allow quantitative evaluation of system performance and insight into individual errors, aiding in improvement and standardization in additive manufacturing. The article provides a comprehensive overview of existing test artifacts, categorized based on geometric features and material used. Various measurement techniques such as stylus profilometry and computed tomography are employed to assess these artifacts. It was shown that Selective Laser Melting (SLM) technology and titanium alloys are prevalent in artifact creation. Specific artifact categories include slits, angular aspects, length parameters, variable surfaces, and others, each accompanied by examples from research literature, highlighting diverse artifact designs and their intended applications. The paper critically discusses the main problems with existing geometries. It paper underscores the importance of user-friendly and unambiguous artifacts for dimensional control, particularly in surface metrology. It anticipates the continued growth of metrological verification in future manufacturing environments, emphasizing the need for precise and reliable measurement results to support decision-making in production conditions

**Key words:** test artifacts, 3D printing, additive manufacturing, surface metrology

## 1. INTRODUCTION

Additive Manufacturing (AM), commonly known as 3D printing, is a process of fabricating objects by layering processed material based on three-dimensional model data. The core of additive manufacturing technologies lies in the successive construction of elements layer by layer, contrasting with subtractive methods where the element is produced through subtractive operations. Multiple AM technologies exist, such as stereolithography, laser sintering, and multi-jet printing, all covered in the international ASTM standard [1].

With the continuous evolution of additive methods, there is a growing need for a deeper understanding of the technology itself by characterizing the quality of the process and, in turn, produced parts. Two approaches to assessing these methods have been defined. The first involves a series of in-situ measurements of components being produced or process characteristics during the fabrication. This method necessitates the placement of additional sensors in the machine workspace, capturing relative positions, orientations, velocities, accelerations or other characteristics of the fabrication process. In the case of AM systems, this approach is often challenging or impossible due to moving elements that are inaccessible to measuring equipment, posing potential hazards associated with

the applied manufacturing technology, such as high-power lasers. The second approach considers measurements of a produced test artifact made in a specific manufacturing system.

Evaluating the performance of manufacturing process by using a real produced test artifact allows an insight into the effect of individual errors in the system which finally contribute to errors in the entire part. The primary advantage of test artifacts is their production, with elements aligning with the real purpose of the system and usually not requiring specialized measuring equipment. In most cases, conventional measuring equipment suffices. The primary goal of a test artifact is to determine the quantitative performance of the system. The advantage of a standardized artifact is its reproducibility in different systems, allowing for relatively easy comparison. With proper and deliberate design, a test artifact can highlight the limitations of the machine itself, becoming a verification method between system users and manufacturers. This facilitates improvements and, consequently, the continuous development of AM methods.

This article provides an overview of existing test artifacts used to characterize AM systems. Additionally, a strategy for standardizing test artifacts to characterize the performance of AM systems is discussed. These principles are supported by existing and published data from the literature, aiming to

\*tomasz.bartkowiak@put.poznan.pl

systematize and compile current achievements related to the verification of additive systems, ultimately allowing for their further development.

## 2. OVERVIEW OF TECHNOLOGIES, MATERIALS AND FEATURES

Additive manufacturing gained its significance in the late 1980s. Stereolithography (SLA) was the first commercially successful technology, followed closely by Fused Deposition Modeling (FDM), Laminated Object Manufacturing (LOM), and Selective Laser Sintering (SLS). As AM advanced, numerous other technologies, such as material spraying, were introduced to the market. The development of stereolithography was linked to the recognition of the standardization of accuracy tests [2]. Consequently, it was acknowledged that a standard test artifact should:

- be large enough to test the manufacturing performance near the printing platform edges,
- include a significant number of small, medium, and large objects with both holes and protruding features,
- have a reasonable creation time for the artifact,
- not consume a large amount of material,
- be „easily” measurable,
- contain geometric features which resemble the real machine parts (e.g.: thin walls, flat surfaces, holes, etc.).

Other researchers strictly adhered to these criteria [3]. Bauza et al. referred to these principles but added that artifacts should contain features along all axes and should include features to determine the minimum achievable size of an element [4]. While many of these features are indeed important for designing a test artifact, it should be noted that an ideal artifact should not only reveal most errors and limitations of the system but also correlate them.

Kruth et al. [5] observed that a test artifact should not only assess system limitations but should also contain information on how to improve the manufacturing process by tuning the technological parameters. Furthermore, Scaravetti et al. stated that artifact verification should not only allow the identification and quantitative determination of defects but primarily determine their sources [6]. Therefore, it was established that a test artifact should additionally:

- have simple geometric shapes enabling clear determination and easy control of geometry,
- not require additional post-processing,
- allow measurements and repeatability analysis.

Moreover, several researchers emphasized the need for the test artifact to include multiples of the same shape to enable measurement repeatability. However, incorporating multiples of the same shape only tests the ability to create the same shape in different locations of the pattern [7]. As different conditions may result in various systematic errors in machine workspace, this leads to differences in the produced shapes in different locations. Therefore, if the system produces multiple artifacts with a high level of repeatability, the shapes created in the same

location in the machine workspace would be exactly the same but in a distorted form.

Although many test artifacts for AM have been proposed in the literature (discussed later in the paper), not all authors adhere to the discussed guidelines, and none of them has undergone a formal standardization procedure. In this paper, we systematize different approaches and highlight differences in geometric features authors focused on in their developed artifacts.

**TABLE 1.** Occurrence of types of artifacts in the literature depending on 3D printing technology

Features Technology	Cylinder	Holes	Angular surfaces	Cracks	Variable surfaces	Cone	Cuboid	Sphere
SLM	[7] [25] [12] [13] [9] [26] [11] [42] [20] [34] [37]	[7] [25] [32] [26] [42] [20] [37] [35]	[31] [12] [13] [16] [9] [11] [10] [19] [20] [21] [22] [34] [18] [23] [24] [35]	[31] [9] [35]	[9] [17]	[7]	[7] [28] [32] [33] [16] [9] [42] [36] [34] [37]	[17] [20] [34]
FDM	[27] [14]	[27] [28]	[27] [28] [16] [14]				[16] [14]	[14]
SLA	[29] [30] [14]	[29] [30]	[30] [16] [14]	[30] [8]		[29] [30]	[29] [30] [16] [14]	[29] [30] [14]
SLS	[29] [30] [14]	[29] [30] [35]	[30] [16] [14] [35]	[30] [8] [35]		[29] [30]	[29] [30] [16] [14]	[29] [30] [14]

Table 1 presents the overview of artifact geometries depending on the manufacturing technology. According to the analyzed literature, the most used printing technology, as indicated by the authors, was Selective Laser Melting (SLM), chosen 53 times. Fused Deposition Modeling (FDM) appeared 11 times, Stereolithography (SLA) 19 times, and Selective Laser Sintering (SLS) 23 times. The most frequently chosen geometries for SLM were angular surfaces (29%), followed by cylindrical artifacts at 20%, cubes at 18%, holes at 15%, slots at 5%, spheres at 5%. surfaces with variable geometries at 4% and cones at 2%.

**TABLE 2.** The occurrence of types of artifacts in the literature depending on the material of manufacture

Features Material	Cylinder	Holes	Angular surfaces	Cracks	Variable surfaces	Cone	Cuboid	Sphere
Nylon	[29] [30] [14]	[29] [30]	[30] [16] [14] [15]	[30]		[29] [30]	[29] [30] [16] [14]	[29] [30] [14]
Acrylate	[27] [30] [14]	[27] [30]	[27] [30] [16] [14]	[30]			[16] [14]	[14]
Stainless steel	[7] [13] [20]	[7] [20] [23]	[13] [16] [20] [23]			[7] [30]	[7] [30] [16]	[7] [30] [20]
ABS/PLA	[30] [14]	[30]	[21] [8] [16] [14]	[21] [8]		[21]	[30] [16] [14]	[30] [14]
Epoxy resin		[28]	[28]				[28]	
Aluminium alloys	[25] [9] [26] [11] [37] [35]	[25] [32] [26] [23] [37] [35]	[31] [16] [9] [23] [35]	[31] [9] [35]	[9]		[32] [33] [16] [9] [37]	
Titanium alloys	[12] [9] [26] [11] [42] [20] [34]	[32] [26] [42] [20]	[12] [16] [9] [11] [10] [19] [20] [21] [22] [34] [18] [24]	[9]	[9] [17]		[32] [16] [9] [42] [36] [34]	[17] [20] [34]

Table 2 illustrates the distribution of the chosen occurrence of artifact geometries based on the printing material according to the analyzed literature. Titanium alloys were the most frequently chosen (35 times), followed by aluminum alloys (26 times). The most chosen geometry for titanium alloys was angular surfaces (34%), followed by cylindrical artifacts at 20%, cubes at 17%, holes at 11%, spheres at 9%. surfaces with variable geometries at 6%, and slots at 3%. Variable surfaces, which can correspond to freeforms and are commonly met in 3D printed parts, do not receive much attention when compared to regular geometries. This especially evident when looking at

the considered technology as only SLM was considered when developing variable surface standards.

Table 3 presents the distribution of the occurrence of measurement techniques in specific literature positions. The authors chose various measurement techniques 62 times in total. Profilometric methods were often selected: optical profilometry 15 times (24%); stylus profilometry 8 times (13%) and laser profilometry 5 times (8%). Other techniques included: coordinate measuring machines (CMM) 11 times (18%); computer tomography 9 times (15%); scanning electron microscopy (SEM) 7 times (11%) and 3D scanners 7 times (11%).

**TABLE 3.** The literature coverage of measurement techniques for measuring elements made with 3D printing

M. method Article	Contact profilometer	Computed tomography	SEM	CMM	Optical profilometer	3D scanner	Laser profilometer
[7]	x			x	x		
[8]	x				x	x	
[9]		x					
[10]	x						
[11]			x		x		
[12]			x		x		
[13]			x				x
[14]				x		x	
[15]		x					
[16]						x	
[17]			x				x
[18]							
[19]						x	
[20]	x	x		x	x	x	x
[21]				x	x		
[22]			x	x	x		
[23]	x	x			x		x
[24]					x	x	
[25]		x		x	x		
[26]			x				
[27]				x			
[28]	x			x			
[29]	x			x			
[30]				x			
[31]				x			
[32]					x		
[33]		x	x		x		
[34]					x	x	x
[35]	x						
[36]		x			x		
[37]		x		x			
[42]		x			x		

### 3. ARTIFACT GEOMETRIES

#### 3.1. Slits.

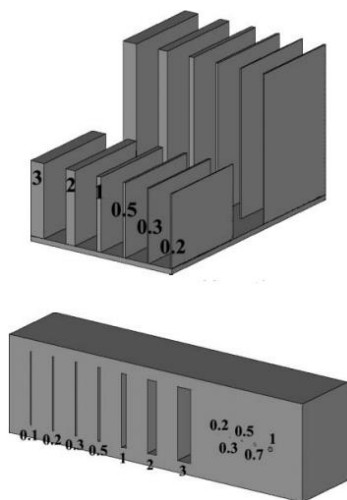


**Fig.1.** Example of a chink standard [8]

The first category of designed artifacts encompasses standards incorporating slit features. Kim et al. devised patterns that take into account two aspects of slits [8]. The first one involves the creation of vertical plates arranged in two rows on a stable base.

The plates in the first row are shorter than those in the second row, maintaining a consistent length for all geometric features. Each pair of plates exhibits a designated difference in thickness (see Fig. 1). The second aspect entails the design of a cuboid with perpendicular slots spanning its entire thickness and varying in widths. The height of the slots remains constant (see Fig. 1).



**Fig.2.** Example of an AMSA 3 compliant chinked pattern [9]

Patterns featuring slit characteristics were also investigated by Townsend et al. [9]. According to their concept, numerous segments were constructed on a circular plan in the form of spatial structures extending from the center to the outer edge, demarcated by slits (Fig. 2.).

#### 3.2. Angular artifacts.

Another category of patterns related to test artifacts involves features representing angular aspects. In their article, Chen et al. proposed printing cuboids positioned at various angles to the machine table within the range of 0 to 90 degrees (Fig. 3.) [10].

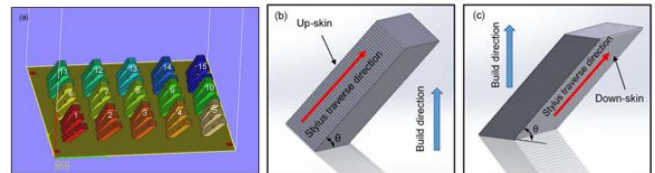


**Fig.3.** Cuboidal test artifacts [10]

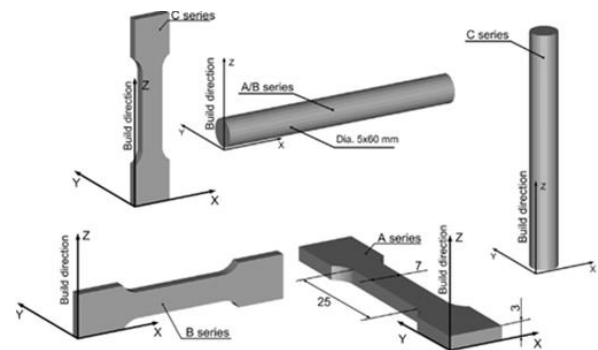


**Fig.4.** Angular positioning of samples for testing the influence of printing direction on tensile strength [11]

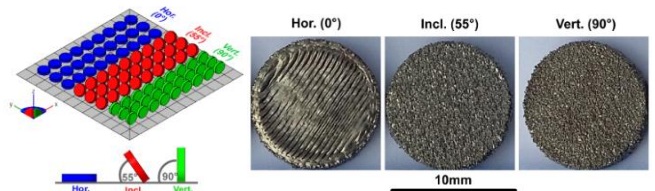


**Fig.5.** Test discs made in one printing series at three angles [12]

On the other hand, Chlebus et al. [11] examined the influence of the orientation of printed tensile test specimen on mechanical strength concerning the direction of printing relative to the table (Fig. 4.).

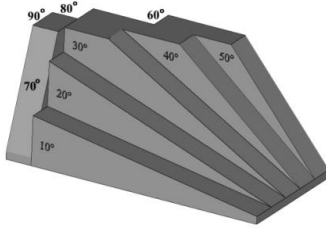


**Fig. 6.** Test artifacts of planes made at an angle to the plane of the printer table [8]

Sidambe et al. proposed test artifacts in the form of disks with the same diameter of 10 mm [12]. The disks were printed at three angular positions: 0°, 55°, and 90°. For each angular position, 27 disks were produced. The author considered it significant to produce all disks in a single printing process. Consequently, a total of 81 disks were printed during one session (Fig. 5.).

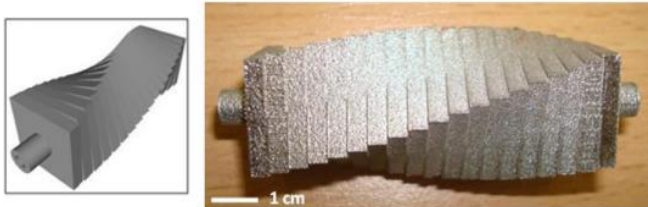


**Fig. 7.** "Truncheon" - a test artifact of planes made at a mutual, relative angle [13]

Kim et al. also conducted research on a compact angular test artifacts [8]. They proposed creating nine rectangular planes, each made at a different incline angle to the printer table within the range of 10° to 90° (with a 10° iteration) (Fig. 6.).

Strano et al. proposed the use of a pattern they called a "truncheon" [13]. It consists of 19 monolithic cuboidal plates with a square base, interconnected and rotated relative to each other in the range of 0° to 90° with a constant iteration (Fig. 7.). Grimm et al. designed a pattern based on the geometry of a sphere [14]. Cuboidal structures with a square base were created on its surface. This resulted in the printing of cuboids at various angles depending on their position relative to the center of the sphere (Fig. 8.). The entire structure is monolithic.

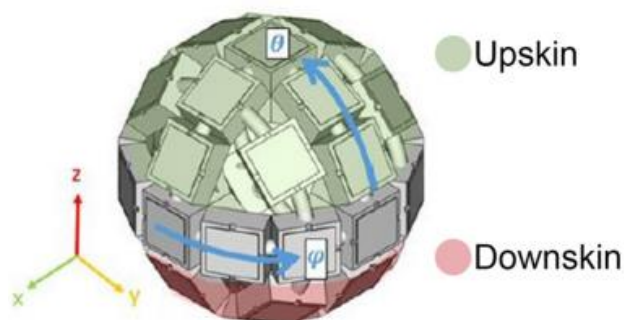


**Fig. 8.** Reference sphere with cuboids marked on its surface [14]

Jansson and Pejryd studied the influence of the orientation of printed tensile bars on mechanical strength relative to the printer table and at different angular positions concerning the reference point – the starting position of printing (Fig. 9.) [15].

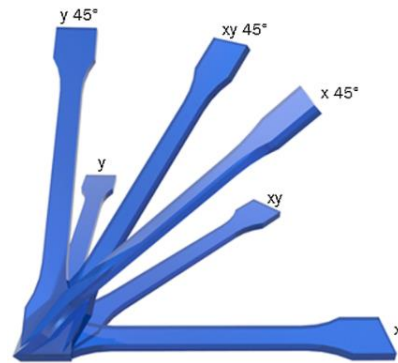


**Fig. 9.** Angular positioning of samples for testing the influence of printing direction on fatigue strength [15]

Moylan, following ASTM F42/ISO TC 261 standards, proposed creating cuboidal plates mounted at different angles on a cylinder (Fig. 10.) [16]. The plates, along with the cylinder, were made monolithically during one printing process.

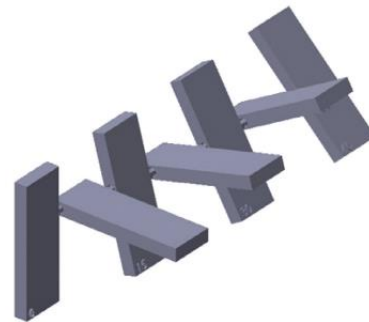


**Fig. 10.** Angle patterns of tiles suspended on a cylinder axis [16]

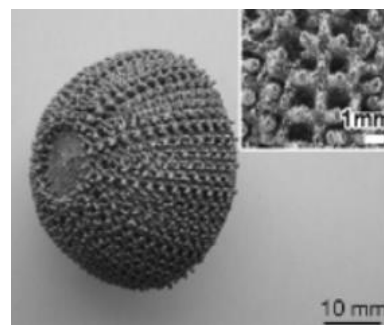


**Fig. 11.** Angle patterns with a lattice structure based on sphere geometry [17]

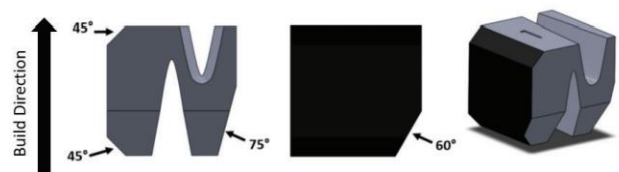


**Fig. 12.** "N" shaped solid standard [18]

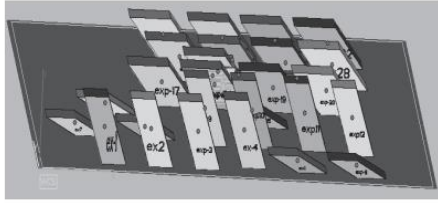


**Fig.13.** Angle plate standard - tilt relative to the Z axis [19]

Zhang et al. proposed creating a structure resembling half of a sphere [17]. Geometric patterns forming a lattice structure were applied to its surface. Depending on the position relative to the center of the sphere, the analyzed area's geometry represented various external structures (Fig. 11.).

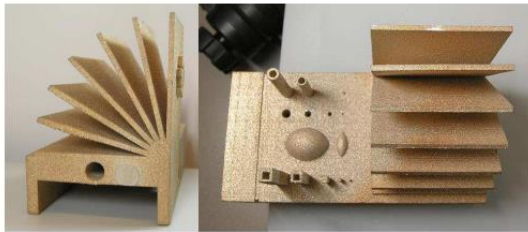


**Fig.14.** Angle standards according to L. Castillo [20]

Eidt et al. created a standard in the shape of the letter "N" [18]. Individual faces of the structure were made at specific angles and orientations to the printer table: 45°; 75°; 60°; 90°. The printing direction was set perpendicular to the base (Fig. 12.). Bacchewar et al. proposed patterns considering a plate-like character [19]. They were positioned at various angles relative to the machine table's position, with the orientation set in relation to the Z-axis (Fig. 13.).

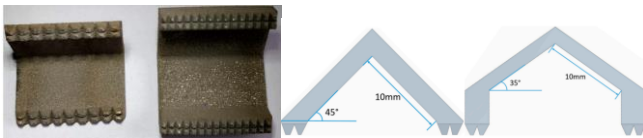


**Fig.15.** "Roof" artifacts [21]

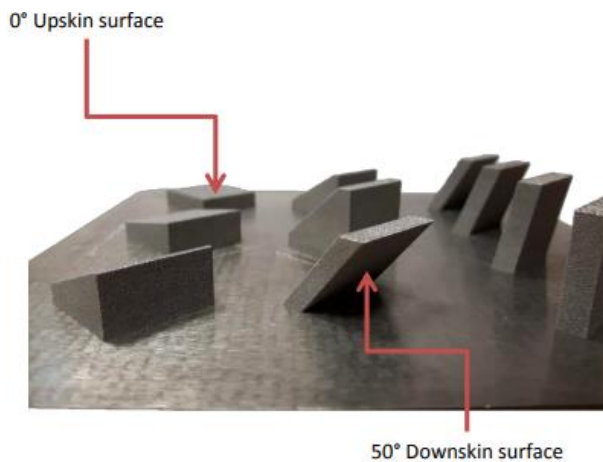


**Fig.16.** Angle plate standard - inclination about different axes [22]

Castillo designed geometric artifacts incorporating multiple geometries in one pattern [20]. The main element consists of 7 plates made at different angles ranging from 0° to 90° (each with a constant 18° iteration). Additionally, the surface pattern

includes two cylinders and two cuboids of different heights with longitudinal holes inside. Five holes of varying diameters and convex parts of spheres were also created (Fig. 14.).

Charles et al. designed "roof" artifacts [21]. The length of the upper surface for both cases was 10 mm. For the first, the inclination of the surface to the horizontal was 45°, and for the second, it was 35°. Additionally, the bases of the roofs end with conical tips (Fig. 15.).

Cabanettes et al., similar to work by P. B. Bacchewar et al., designed angular plate artifacts [22]. They also proposed using different plate shapes and angular positions relative to other axes (Fig. 16.).

Delgado et al. proposed creating artifact shapes with a cross-sectional profile of a rectangular trapezoid [23]. A through-hole was designed through the center of each structure. Each shape was produced on a different side relative to the printer table (Fig. 17.).

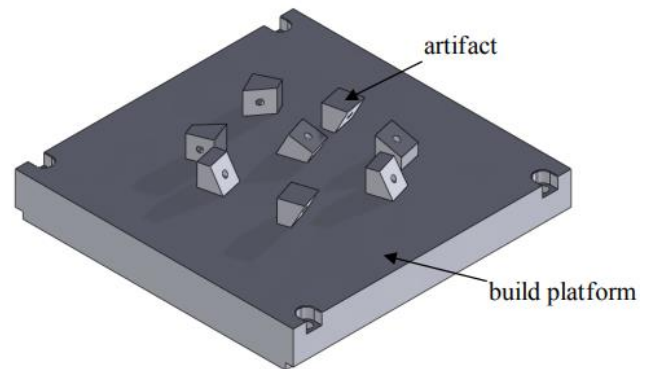


**Fig.17.** Solid artifacts on the longitudinal section of a rectangular trapezoid [23]

Triantaphyllou et al. created artifacts based on a plate construction [24]. The designed geometries were formed in the range from 0° to 90° at 30° intervals. The first group was printed on a monolithic base, while the second was printed without it – as a thin-walled plate (Fig. 18.).

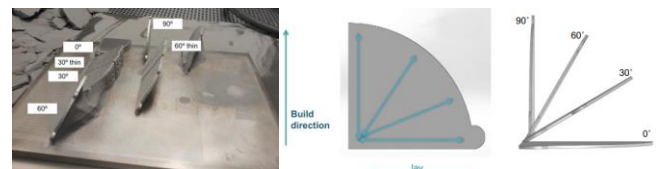


**Fig.18.** Angular plate artifacts [24]

### 3.3. Variable surfaces.

Townsend et al. were the first to address the issue associated with producing variable surface geometries using additive technologies [9]. Consequently, they proposed artifacts based on trigonometric functions, including sinusoidal functions with a decreasing period for increasing arguments (Fig. 19.a)). To accurately replicate possible manufacturing scenarios for variable surface geometries, it proved necessary to employ the production of integral artifact cubes with internally generated surfaces of varying geometry in different angular orientations (Fig. 19.b)).

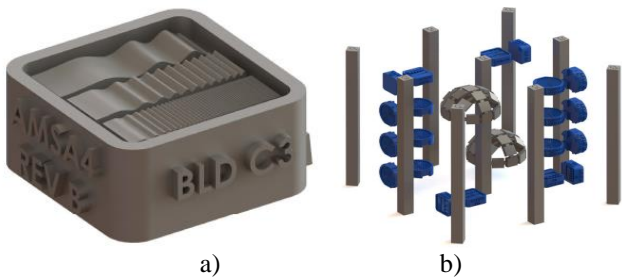


Fig.19. A standard of variable surface geometries [9]

### 3.4. Artifacts related to the length parameter.

Townsend et al. also dealt with artifacts related to replicating length parameters [25]. They suggested producing two cylinders of different diameters connected with bases that form a monolithic structure. The smaller cylinder was defined at the base as a circle with a diameter of 3 mm and a length of 4 mm, fully filled with material throughout the cross-section. Meanwhile, the larger cylinder had an internal diameter greater than 3 mm and a length greater than 4 mm, featuring a non-through hole with a diameter of 3 mm at its center. The verification of length involved checking the outer diameter at various distances from the base of the smaller cylinder (0.50 mm, 1.25 mm, 2 mm, 2.75 mm). For the larger cylinder, the inner diameter dimension was checked at the same distances

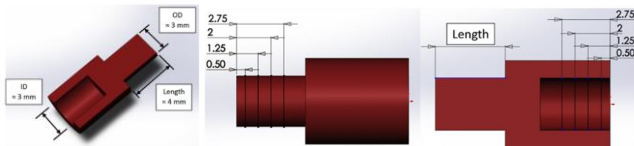


Fig.20. Length artifacts based on cylinder construction [25]

from its base (Fig. 20.).

Similarly to variable surface artifacts, Townsend et al. proposed test cubes with specific length geometries [9]. The cubes were produced at different angular positions, featuring three types of artifacts: a series of cylinders, an inclined surface, and a flat surface (Fig. 21.). Verification is based on surface distance measurements or a given cylinder.



Fig.21. Length artifacts: cylinders, angular surface, flat surface [9]

Danilevicius et al. proposed artifacts based on the geometric structure of chainmail [26]. Toroidal bodies were interconnected by mutual interlocking with each adjacent block. The internal diameter was designed to be 27  $\mu\text{m}$  with a wall thickness of 3.5  $\mu\text{m}$ . Subsequently, the mutual positions of the toroids and the geometric dimensions of the bodies were checked (Fig. 22.).

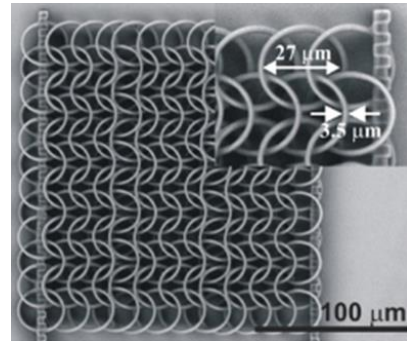


Fig.22. Length artifacts based on the geometric structure of chainmail [26]

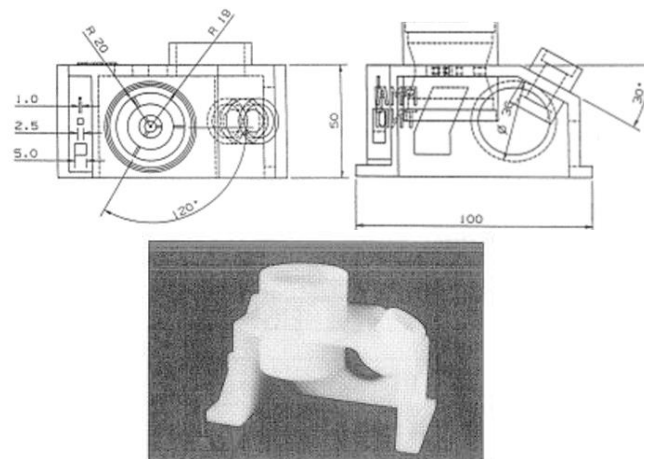


Fig.23. Kruth's test artifact [27]

### 3.5. Multiple feature artifacts.

J. P. Kruth, one of the pioneers of additive technologies over 40 years ago, drew attention to the emerging problem of verifying quality and studying the influences of executed geometries on the quality of the product [27]. He initiated the creation and design of test artifacts, proposing an artifact containing multiple geometries based on the most commonly manufactured shapes. This included internal holes of varying

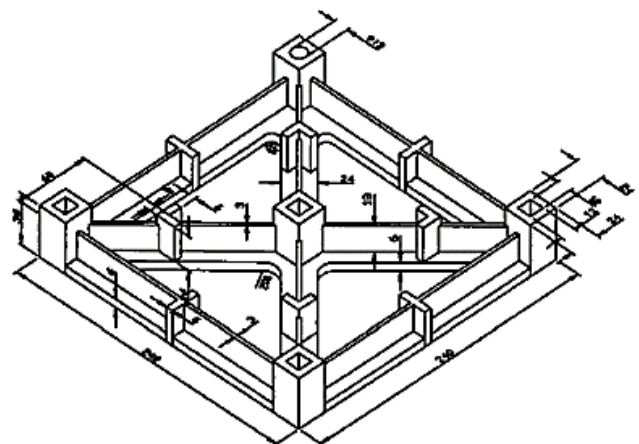
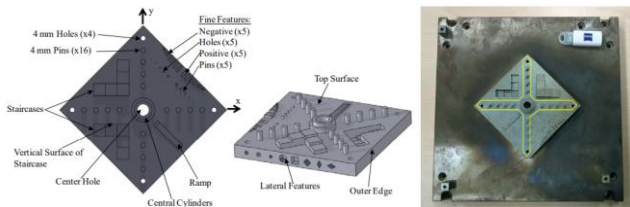


Fig.24. Gargiulo's artifact [28]

diameters, distances between individual surfaces, and slots of different sizes (Fig. 23.).

Ippolito et al. study mention Gargiulo's artifact [28]. It consists of the construction of four interconnected rectangular prisms with square-section holes connected by six plates. Each plate and rectangular prism has a defined, specific geometry and dimensions subject to verification (Fig. 24.). Moylan et al. proposed a single test pattern with applied artifacts of different geometries [7]. Various holes were considered, including circular, square, and trapezoidal shapes. Additionally, cylindrical pins, stepped geometries (concave and convex), and slots of varying widths were created. The entire structure was embedded on a square plate, with some of the holes crossing the plate transversely (Fig. 25.).



**Fig.25.** Artifacts with diverse geometries in one test pattern [7]

Fahad and Hopkinson designed a pattern based on solids: cylinders, cones, cubes, hemispheres, and triangular-based prisms [29]. The solids were produced on different sides in different positions on the base plate. In some geometries, through-holes with a circular cross-section were implemented (Fig. 26.).

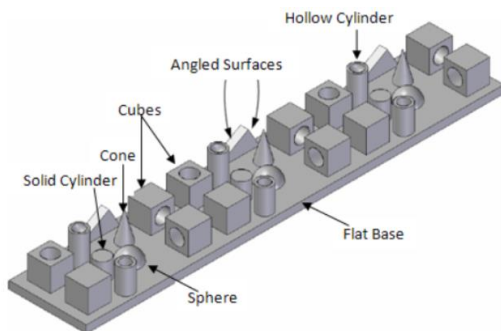


**Fig.26.** Test standard by M. Fahad and N. Hopkinson [29]

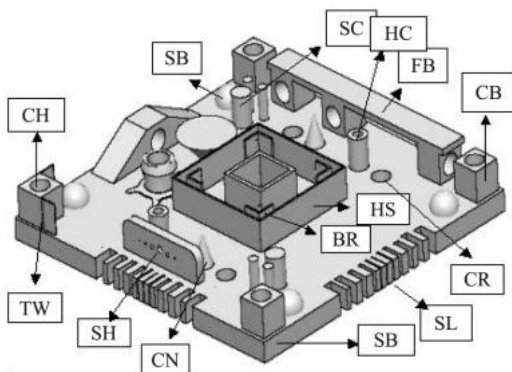


**Fig.27.** Artifacts with various geometries in one test pattern according to M. Mahesh et al. [30]

Mahesh et al. [30] proposed a similar pattern concept to the work by Moylan et al. [7]. The artifacts were all placed on a square plate, featuring inclined surfaces, stepped

constructions, or holes with different cross-sections. Slots were also implemented on the lateral surfaces of the base plate (Fig. 27.).

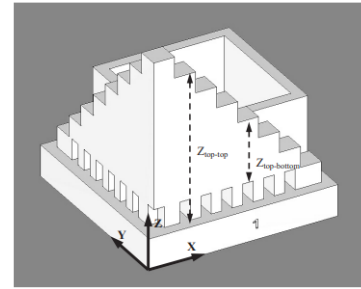


**Fig.28.** Step artifacts [31]

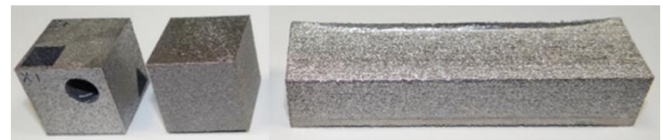


**Fig.29.** Cubic and cuboid test artifact [32]

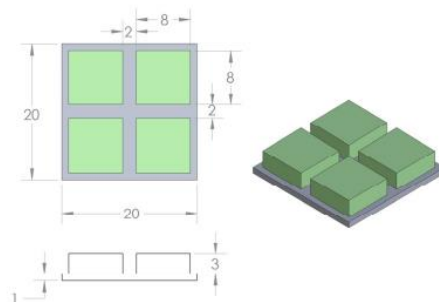


**Fig.30.** Cuboidal Test Artifact – Series 4 [33]

Sercombe and Hopkinson designed a test pattern based on stepped artifacts [31]. The stepped geometries converge at right angles, each consisting of eight steps of identical dimensions. Additionally, in the spaces under the stepped geometry, slots were included, six on each side. The entire structure was placed on a cubic stable base (Fig. 28.).

Gomez et al. used an artifact for surface quality verification, consisting of a cubic block with a non-through hole and a longitudinal rectangular prism made of solid material [32] (Fig. 29.).

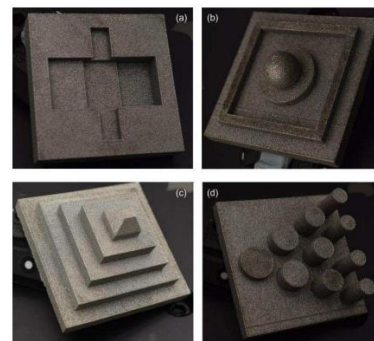


**Fig.31.** Set of test artifacts according to D. Sims-Waterhouse et al. [34]

Roberts et al. used plate artifacts with dimensions of 8 mm x 8 mm x 3 mm [33]. A series of test patterns were made with

four pieces on a monolithic plate. Distances between individual artifacts were 2 mm, and the overall dimensions of the plate were 20 mm x 20 mm (Fig. 30.).

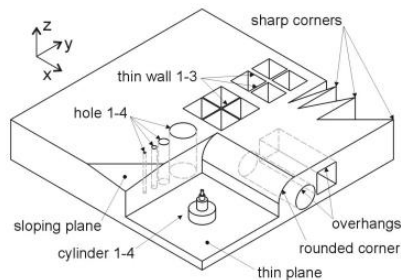


**Fig.32.** Comprehensive test pattern with various artifact geometries according to J. P. Kruth et. al. [35]

Sims-Waterhouse et al. proposed the creation of four types of artifacts [34]. In the first (Fig. 31. a)), a concave geometric character was considered, consisting of five rectangular prisms made as recesses in the material at different depths. In the second (Fig. 31. b)), a sphere was planned in the center of a plate surrounded by a rectangular prism frame. The third (Fig. 31. c)) featured a stepped character based on pyramid geometry. Finally, in the fourth (Fig. 31. d)), cylindrical pins of different base diameters and heights were created.

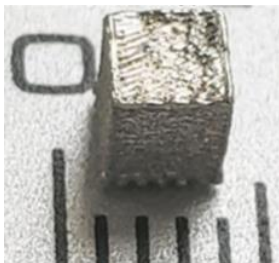


**Fig.33.** Cubic artifact [36]

Kruth et al. also proposed a comprehensive test pattern containing various artifact geometries [35]. In addition to creating cylinders and holes (in cross-section and along the length) with different diameters, sharp corners were designed at various angles in the cross-section of the base plate. Additionally, non-through holes with a square cross-section were proposed in very close proximity to each other. This allowed verification of the realization of the thinness of neighboring walls (Fig. 32.).

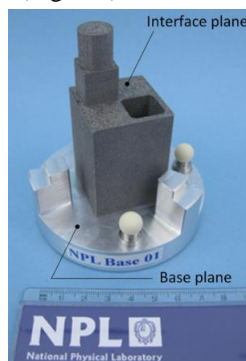


**Fig.34.** NPL Base 01 test standard [37]

Liu [36], like Gomez et al., used a cubic block with dimensions of 4 mm x 4 mm x 4 mm (Fig. 33.).

Lou et al. proposed a pattern consistent with NPL Base 01 [37]. The base consists of a flat base surface forming the top surface of a durable structural alloy. A square cross-section hole with rounded corners was made in the structure. Additionally, a smaller rectangular prism in the corner and a cylinder of the same height on top of it were created on the base surface (Fig. 34.).

#### 4. DISCUSSION

In this work, we demonstrated the abundance of features and layouts of surface metrology artifacts. We showed that majority of them were mainly designed for form evaluation using CMM or 3D scanning. There is no single artifact that can be used for form and surface topography evaluation and all measurement techniques: tactile and optical profilometry, optical microscopy, SEM, CMM, light and microCT scanning. There are inherent physical differences between surface acquisition methods which result in different vertical and horizontal measurement resolution or voxel size and ability to credibly represent the specific geometric features (e.g. steep slopes, high curvature spikes or pores) [38]. In terms of optical microscopy, coherence scanning interferometry (CSI) exhibit superior vertical resolution but high numerical aperture (NA) cannot be applied, which poses challenges in reconstructing smooth surfaces characterized by steep local slopes [39]. Confocal laser scanning microscopy (CLSM) addresses this challenge by employing high NA objectives, enabling it to measure steeper slopes compared to CSI. However, the resolution of height measurements is contingent upon the NA value. Consequently, lower height resolution may result when using low-magnification optics typically associated with low NA. Therefore, CLSM may not be suitable for smooth surfaces requiring measurement at low magnification. Conversely, for rough surfaces, CLSM yields notably superior outcomes compared to CSI. Nonetheless, when assessing extremely rough surfaces, particularly those with pronounced tilt or spherical characteristics, subpar results may arise, such as the occurrence of "ghost points" due to surface multi-reflection [40]. In such scenarios, the focus variation (FV) technique presents a more effective solution, leveraging texture information from bright field images. However, this approach sacrifices height resolution compared to CLSM, contingent upon factors such as texture contrast, the specific algorithm for focus position extraction, numerical aperture, and wavelength. Contact profilometry is an alternative but does not allow to measure surfaces with high Rz (maximum peak to valley height of the profile) or concave or convex form of high curvature or step-like slopes. This reduces the number of applications where this technique can be applied.

Other factor is the presence of re-entrant features [41] which are a signature of additive manufacturing that involves polymer- or metal-based powders as input material. Those kinds of features cannot be accurately measured using other than by X-ray micro-computed tomography. Large scale re-entrants can be acquired, to some extent, with 3D scanning but this limits the characterization to form. On the other hand, microCT has its



limitations. To achieve high resolution measurement, which can correspond to lateral resolution of optical microscopy, the thickness of the measured material is limited. The smaller the voxel size, the lower the power X-ray radiation which can be applied what limits the material penetration performance. This excludes large artifacts from surface analysis by that method. MicroCT is also the only non-destructive alternative to measure internal cavities or holes.

There are a few artifacts that can be used as benchmark tool to evaluate the quality of additive manufacturing process which can be also used a metrological test for all measurement techniques. Those artifacts involve thin flat surfaces which can be inclined at various built-up angles. Multi-feature parts, as in section 3.5, cannot be precisely measured by microCT due to the size of the artifacts. The presence of cylindrical or variable surfaces limits the tactile profilometry to only a single scanning direction. The surface topography of internal features cannot be precisely measured unless surrounding wall thickness is low. The above issues may lead to the statement that there is no standard artifact that can be called universal in terms of manufacturing and metrology. The unification of the geometries and features should come but with respect to a clear limitation to the certain AM technologies and specific measurement techniques.

## 5. CONCLUSIONS

The article discusses the pivotal role of test artifacts in improving production by establishing geometric and dimensional control. It presents the main features of artifacts, encompassing standard objects with simple geometries (cubes, rectangular prisms, etc.) and specific methods for specialized applications. Additionally, the article provides guidelines regarding the design, purpose, and utilization of individual dimensional artifacts. Emphasis is placed on underscoring the impact and significance of test artifacts, which remain fundamental for the verification and calibration of machines and technological processes.

The article notes the importance of these artifacts being user-friendly, suitable for operation in challenging conditions, and unambiguous in interpreting results. In the field of surface metrology, there is a need to develop methods and artifacts for determining the fidelity of topography, especially in additive manufacturing processes involving complex surfaces and angles. Parts produced using additive manufacturing methods with hidden or internal features pose contemporary measurement challenges, prompting the development of new artifact solutions tailored to specific tasks, AM technology and most important to specific measurement technology or technologies.

The article also addresses issues related to the materials used in designing and creating test patterns, emphasizing that authors often align the measurement method with the manufacturing material. Such an approach enables the creation of dedicated solutions that meet both technological and verification needs. Similarly, geometric considerations in artifact design are shaped by the material and the printing technology itself. This

directly influences the quality of standards and their subsequent usefulness in verification.

The authors anticipate that in future manufacturing environments, the importance of metrological verification and the certainty of measurement results will continue to grow. Advanced technologies based on automation require precise and reliable information about the components being manufactured. Only when significant functional features of components are measured with specified uncertainties can appropriate decisions be made regarding compliance with production conditions.

## FUNDING

Publication was financed by the Polish state budget under the Polish Metrology program of the Ministry of Education and Science; project title: "Surface metrology in additive manufacturing", no PM/SP/0077/2021/1, co-financing amount PLN 999,900.00, total project value PLN 999,900.00.

## REFERENCES

- [1] ASTM Standard F2792, "Terminology for Additive Manufacturing Technologies," *ASTM International*, 2012, doi: 10.1520/f2792-12.
- [2] J. Richter and P. F. Jacobs, *Accuracy in Rapid Prototyping & Manufacturing*. Society of Manufacturing Engineers, 1992, pp. 287–315.
- [3] B. Hao, E. Korkmaz, B. Bediz, and O. B. Ozdoganlar, "A Novel Test Artifact for Performance valuation of Additive Manufacturing Processes," *Engineering, Materials Science*, 2014, doi: Corpus ID: 6795632.
- [4] M. B. Bauza *et al.*, "Study of accuracy of parts produced using additive manufacturing," *ASPE Spring Topical*, pp. 86–91, 2014.
- [5] J.-P. Kruth, M. C. Leu, and T. Nakagawa, "Progress in Additive Manufacturing and Rapid Prototyping," *CIRP Annals*, vol. 47, no. 2, pp. 525–540, 1998, doi: 10.1016/s0007-8506(07)63240-5.
- [6] D. Scaravetti, P. Dubois, and R. Duchamp, "Qualification of rapid prototyping tools: proposition of a procedure and a test part," *The International Journal of Advanced Manufacturing Technology*, vol. 38, no. 7–8, pp. 683–690, 2007, doi: 10.1007/s00170-007-1129-2.
- [7] S. Moylan, J. Slotwinski, A. Cooke, K. Jurrens, and M. A. Donmez, "An Additive Manufacturing Test Artifact," *Journal of Research of the National Institute of Standards and Technology*, vol. 119, p. 429, 2014, doi: 10.6028/jres.119.017.
- [8] G. D. Kim and Y. T. Oh, "A benchmark study on rapid prototyping processes and machines: Quantitative comparisons of mechanical properties, accuracy, roughness, speed, and material cost," *Proceedings of the Institution of Mechanical Engineers, Part B: Journal of Engineering Manufacture*, vol. 222, no. 2, pp. 201–215, 2008, doi: 10.1243/09544054jem724.
- [9] A. Townsend, N. Senin, L. Blunt, R. J. K. Leach, and J. S. Taylor, "Surface texture metrology for metal additive manufacturing: a review," *Precision Engineering*, vol. 46, pp. 34–47, 2016, doi: 10.1016/j.precisioneng.2016.06.001.
- [10] Z. Chen, X. Wu, D. Tomus, and C. H. J. Davies, "Surface roughness of Selective Laser Melted Ti-6Al-4V alloy components," *Additive Manufacturing*, vol. 21, pp. 91–103, 2018, doi: 10.1016/j.addma.2018.02.009.
- [11] E. Chlebus, B. Kuźnicka, T. Kurzynowski, and B. Dybała, "Microstructure and mechanical behaviour of Ti-6Al-7Nb alloy produced by selective laser melting," *Materials Characterization*, vol. 62, no. 5, pp. 488–495, 2011, doi: 10.1016/j.matchar.2011.03.006.
- [12] A. T. Sidambe, "Three dimensional surface topography characterization of the electron beam melted Ti6Al4V," *Metal Powder Report*, vol. 72, no. 3, pp. 200–205, 2017, doi: 10.1016/j.mprp.2017.02.003.
- [13] G. Strano, L. Hao, R. M. Everson, and K. E. Evans, "Surface roughness analysis, modelling and prediction in selective laser

- melting,” *Journal of Materials Processing Technology*, vol. 213, no. 4, pp. 589–597, 2013, doi: 10.1016/j.jmatprotec.2012.11.011.
- [14] T. Grimm, G. Wiora, and G. Witt, “Characterization of typical surface effects in additive manufacturing with confocal microscopy,” *Surface Topography: Metrology and Properties*, vol. 3, no. 1, p. 014001, 2015, doi: 10.1088/2051-672x/3/1/014001.
- [15] A. Jansson and L. Pejryd, “Characterisation of carbon fibre-reinforced polyamide manufactured by selective laser sintering,” *Additive Manufacturing*, vol. 9, pp. 7–13, 2016, doi: 10.1016/j.addma.2015.12.003.
- [16] S. Moylan, “Progress toward standardized additive manufacturing test artifacts,” in *ASPE*, 2015, pp. 100–105.
- [17] L. C. Zhang, D. Klemm, J. Eckert, Y. L. Hao, and T. B. Sercombe, “Manufacture by selective laser melting and mechanical behavior of a biomedical Ti–24Nb–4Zr–8Sn alloy,” *Scripta Materialia*, vol. 65, no. 1, pp. 21–24, 2011, doi: 10.1016/j.scriptamat.2011.03.024.
- [18] W. Edit, E. Tatman, J. McCarther, J. Kastner, S. Gunther, and J. Gockel, “Surface roughness characterization in laser powder bed fusion additive manufacturing,” presented at the 30th Annual International Solid Freeform Fabrication Symposium – An Additive Manufacturing Conference, 2019.
- [19] P. B. Bacchewar, S. K. Singhal, and P. M. Pandey, “Statistical modelling and optimization of surface roughness in the selective laser sintering process,” *Proceedings of the Institution of Mechanical Engineers, Part B: Journal of Engineering Manufacture*, vol. 221, no. 1, pp. 35–52, 2007, doi: 10.1243/09544054jem670.
- [20] L. Castillo, “Study about the rapid manufacturing of complex parts of stainless steel and titanium,” TNO report with the collaboration of AIMEE, 2005.
- [21] A. Charles, A. Elkaseer, L. Thijs, V. Hagenmeyer, and S. Scholz, “Effect of Process Parameters on the Generated Surface Roughness of Down-Facing Surfaces in Selective Laser Melting,” *Applied Sciences*, vol. 9, no. 6, p. 1256, 2019, doi: 10.3390/app9061256.
- [22] F. Cabanettes *et al.*, “Topography of as built surfaces generated in metal additive manufacturing: A multi scale analysis from form to roughness,” *Precision Engineering*, vol. 52, pp. 249–265, 2018, doi: 10.1016/j.precisioneng.2018.01.002.
- [23] “Studying the repeatability in DMLS technology using a complete geometry test part,” in *Innovative Developments in Design and Manufacturing*, CRC Press, 2009, pp. 367–372. Accessed: Mar. 22, 2024. [Online]. Available: <http://dx.doi.org/10.1201/9780203859476-63>
- [24] B. Cavallini, J. Ciorana, C. Reguant, and J. Delgado, “Studying the repeatability in DMLS technology using a complete geometry test part,” in *Innovative Developments in Design and Manufacturing*, CRC Press, 2009. [Online]. Available: <http://dx.doi.org/10.1201/9780203859476.ch54>
- [25] A. Townsend, L. Pagani, P. Scott, and L. Blunt, “Areal surface texture data extraction from X-ray computed tomography reconstructions of metal additively manufactured parts,” *Precision Engineering*, vol. 48, pp. 254–264, 2017, doi: 10.1016/j.precisioneng.2016.12.008.
- [26] P. Danilevičius *et al.*, “Laser 3D micro/nanofabrication of polymers for tissue engineering applications,” *Optics & Laser Technology*, vol. 45, pp. 518–524, 2013, doi: 10.1016/j.optlastec.2012.05.038.
- [27] J. P. Kruth, “Material Ingress Manufacturing by Rapid Prototyping Techniques,” *CIRP Annals*, vol. 40, no. 2, pp. 603–614, 1991, doi: 10.1016/S0007-8506(07)61136-6.
- [28] R. Ippolito, L. Iuliano, and A. Gatto, “Benchmarking of Rapid Prototyping Techniques in Terms of Dimensional Accuracy and Surface Finish,” *CIRP Annals*, vol. 44, no. 1, pp. 157–160, 1995, doi: 10.1016/S0007-8506(07)62296-3.
- [29] M. Fahad and N. Hopkinson, “Evaluation and comparison of geometrical accuracy of parts produced by sintering-based additive manufacturing processes,” *The International Journal of Advanced Manufacturing Technology*, vol. 88, no. 9–12, pp. 3389–3394, 2016, doi: 10.1007/s00170-016-9036-z.
- [30] M. Mahesh, Y. S. Wong, J. Y. H. Fuh, and H. T. Loh, “Benchmarking for comparative evaluation of RP systems and processes,” *Rapid Prototyping Journal*, vol. 10, no. 2, pp. 123–135, 2004, doi: 10.1108/13552540410526999.
- [31] T. B. Sercombe and N. Hopkinson, “Process Shrinkage and Accuracy during Indirect Laser Sintering of Aluminium,” *Advanced Engineering Materials*, vol. 8, no. 4, pp. 260–264, 2006, doi: 10.1002/adem.200500265.
- [32] C. Gomez, R. Su, A. Thompson, J. DiSciaccia, S. Lawes, and R. Leach, “Optimization of surface measurement for metal additive manufacturing using coherence scanning interferometry,” *Optical Engineering*, vol. 56, no. 11, p. 111714, 2017, doi: 10.1117/1.oe.56.11.111714.
- [33] C. E. Roberts, D. Bourell, T. Watt, and J. Cohen, “A Novel Processing Approach for Additive Manufacturing of Commercial Aluminum Alloys,” *Physics Procedia*, vol. 83, pp. 909–917, 2016, doi: 10.1016/j.phpro.2016.08.095.
- [34] D. Sims-Waterhouse, P. Bointon, S. Piano, and R. K. Leach, “Experimental comparison of photogrammetry for additive manufactured parts with and without laser speckle projection,” in *Optical Measurement Systems for Industrial Inspection X*, 2017. Accessed: Mar. 22, 2024. [Online]. Available: <http://dx.doi.org/10.1117/12.2269507>
- [35] D. Sims-Waterhouse, P. Bointon, S. Piano, and R. K. Leach, “Experimental comparison of photogrammetry for additive manufactured parts with and without laser speckle projection,” in *Optical Measurement Systems for Industrial Inspection X*, 2017. Accessed: Mar. 22, 2024. [Online]. Available: <http://dx.doi.org/10.1117/12.2269507>
- [36] W. Liu, “Optical and XCT Measurement of Additively Manufactured Surfaces,” *Fields: journal of Huddersfield student research*, vol. 7, no. 1, 2021, doi: 10.5920/fields.803.
- [37] A. Triantaphyllou *et al.*, “Surface texture measurement for additive manufacturing,” *Surface Topography: Metrology and Properties*, vol. 3, no. 2, p. 024002, 2015, doi: 10.1088/2051-672x/3/2/024002.
- [38] Y. Zou, J. Li, and Y. Ju, “Surface topography data fusion of additive manufacturing based on confocal and focus variation microscopy,” *Optics Express*, vol. 30, no. 13, p. 23878, Jun. 2022, doi: 10.1364/oe.454427.
- [39] A. Matilla, J. Mariné, J. Pérez, C. Cadevall, and R. Artigas, “Three-dimensional measurements with a novel technique combination of confocal and focus variation with a simultaneous scan,” in *SPIE Proceedings*, 2016. Accessed: Mar. 22, 2024. [Online]. Available: <http://dx.doi.org/10.1117/12.2227054>
- [40] R. Leach, *Optical Measurement of Surface Topography*. Springer Science & Business Media, 2011.
- [41] T. Bartkowiak, B. Gapiński, M. Wiczorowski, P. Mielniński, and C. A. Brown, “Capturing and characterizing geometric complexities of metal additively manufactured parts using x-ray micro-computed tomography and multiscale curvature analyses,” *Surface Topography: Metrology and Properties*, vol. 11, no. 1, p. 014002, 2023, doi: 10.1088/2051-672x/acb3e7.
- [42] A. Townsend *et al.*, “An interlaboratory comparison of X-ray computed tomography measurement for texture and dimensional characterisation of additively manufactured parts,” *Additive Manufacturing*, vol. 23, pp. 422–432, 2018, doi: 10.1016/j.addma.2018.08.013.